How the atomic structure of a crystal can be seen without a high-resolution microscope

V. L. Indenbom
Institute of Crystallography, Academy of Sciences, Moscow, Russia

S. B. Tochilin
Oxford University, Oxford, England

(Submitted 29 June 1995)
Pis'ma Zh. Éksp. Teor. Fiz. **62**, No. 3, 252–255 (10 August 1995)

The method of high-resolution electron microscopy (HREM) has been widely used in the last few years to study the atomic structure of crystalline materials and crystal lattice defects. The possibilities of HREM are limited by spherical aberration. As a result, even the best microscopes have a resolution of no better than 1–2 Å, i.e., much greater than the electron wavelength, which for characteristic values of the accelerating voltage 0.1–1.0 MeV reaches 0.038 and 0.012 Å, respectively. The resolution can be increased by 1.5 orders of magnitude by using, instead of HREM, dynamic electron diffraction patterns and by investigating not only the coordinates of the reflections, but also how the average intensity of the reflections along the radius of the electron diffraction pattern decreaes (primarily the width of the electron diffraction pattern, which determines the width of the peaks of the Bloch waves on the exit surface of the transilluminated foil). As an example, a resolution of the order of 0.10 Å is given for gold with transmission along ⟨111⟩. © *1995 American Institute of Physics.*

In the case of dynamic electron diffraction the channeling of electrons along atomic chains which are oriented parallel to the transmission direction has the greatest effect on the character of the electron wave field $\psi(x,y)$ on the exit surface of the foil.[1] The wave field $\psi(x,y)$ usually consists of weakly overlapping $1S$-type Bloch waves which, channel along atomic chains parallel to the transmission direction and which are localized on these chains within $\rho = 2\hbar^2/mZe^2$, where m is the relativistic mass of an electron, e is the electron charge, and Z is the atomic number of the atoms or ions comprising the chain.[2–4]

The free propagation of this wave field

$$\psi(xy) = \sum_{m,n} \psi_{1S}(x - m\mathbf{a}, y - n\mathbf{b}) \tag{1}$$

in free space gives the dynamic electron diffraction pattern

$$\tilde{\psi}(k_x, k_y) = \sum_{m,n} \tilde{\psi}_{1S}(k_x - m\mathbf{a}^*,\ k_y - n\mathbf{b}^*) \tag{2}$$

(the phases of all chains, including the chains shifted along the z axis, are identical because only the zeroth Laue zone is excited, and the lattice potential is averaged along the direction of channeling). In Eqs. (1) and (2) **a** and **b** are parameters and $m\mathbf{a}$ and $n\mathbf{b}$ are the translation vectors of the network of chains in the (x,y) plane; $\mathbf{a}^*$ and $\mathbf{b}^*$ are parameters and $m\mathbf{a}^*$and $n\mathbf{b}^*$are reciprocal-lattice vectors; and, $\tilde{\psi}_{1S}(k_x, k_y)$ is the Fourier transform of the Bloch function ψ_{1S}.

In the screened Coulomb potential approximation the Bloch waves ψ_{1S} for separate atomic chains have the form[2,4] (the normalization factor is dropped)

$$\psi_{1S}(r)=\exp(-2r/\rho), \tag{3}$$

where $r=\sqrt{x^2+y^2}$ is the distance from the atomic chain and

$$\rho=(\hbar^2 d)/mZe^2 a_{TF}; \tag{4}$$

here d is the distance between the atoms in a chain, and a_{TF} is the Thomas–Fermi screening radius:

$$a_{TF}=0.885\hbar^2/m_0 e^2 Z^{1/3}, \tag{5}$$

and m_0 is the electron rest mass. It should be noted that the parameter ρ describes all characteristics of the lattice and the conditions of irradiation, including the accelerating voltage $U=(m-m_0)c^2/e$.

The screened Coulomb potential approximation was developed in application to the channeling of high-energy electrons,[5] when many bound (channeled) Bloch waves arise. It can be shown, however, that this approximation is valid under conditions of electron diffraction and high-resolution electronic microscopy, when one and two (only for heavy chains) bound Bloch waves appear.

According to Ref. 4 , the number N of bound Bloch states with negative energy $E_\perp$ of the transverse electron motion can be estimated by joining the Bloch waves midway between the neighboring chains. This condition gives

$$(2N-1)^2 \leqslant d_\perp/\rho, \tag{6}$$

where $d_\perp$ is the distance between neighboring chains. The estimate (6), which takes into account exactly the shape of the potential well in the Schrödinger equation, differs advantageously in this respect from the well-known estimate obtained by Fujimoto *et al.*[1] on the basis of an analysis of a square potential well. It follows from relation (6) that if $d_\perp \geqslant 9\rho$, there is only one channeled $1S$ Bloch wave; if $d_\perp \geqslant 25\rho$, there are only two channeling $1S$ and $2S$ Bloch waves, and if $d_\perp \geqslant 49\rho$, there are only three channeling $1S$, $2S$, and $3S$ Bloch waves, which is impossible even for heavy atoms. The most common case is $N \leqslant 2$, i.e., $d_\perp \geqslant 9\rho$; according to Ref. 4, this case corresponds to $-E_\perp \geqslant (2m)^{-1}[(N-1/2\hbar\rho]$, i.e., the condition $-E_\perp \geqslant (2m)^{-1}(3/2\hbar\rho)^2$, or the condition on the extinction length $L_{2S} \geqslant 16\lambda mE/3\hbar\rho$, where λ is the electron wavelength. We will therefore restrict the discussion to the case $N=1$, where only one coupled (channeling) $1S$ Bloch wave is excited.

The estimates employed above were based on the screened Coulomb potential approximation, which makes it possible to describe Bloch waves in analytic form without any numerical calculations. In Fig. 1 the case of a $1S$ Bloch wave in gold is studied as an

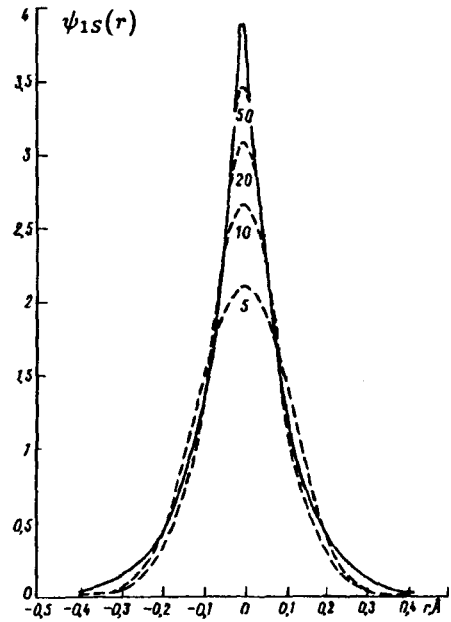

FIG. 1. $1S$ Bloch wave in gold, 400 keV, transmission along $\langle 111 \rangle$. The solid line — 2527 plane waves in the matrix calculation — corresponds virtually exactly to the approximation (3). The dashed curves are the results of approximate matrix calculations. The numbers on the curves are the rank of the matrix. Explanations are given in the text. The case, of gold with tranmission along $\langle 001 \rangle$ studied by Vergasov,[6] corresponds to 81 plane waves with a matrix rank of only 14.

illustration. According to Vergasov,[6] despite the high transverse energy $E_\perp = -169$ eV, such a wave should have a half-width of the order of 0.4 Å and should overlap appreciably with the waves centered on neighboring chains. It follows from Fig. 1, however, that nothing like this actually happens: As the rank of the dynamic matrix increases in the calculation and an increasingly larger number of plane and Bloch waves come into play, the true form of the $1S$ wave, which coincides with the above-indicated simple formula (3), comes through. The half-width of ψ_{1S} is found to be 0.10 Å.

Having verified the validity of our approximation, we note that in this approximation the $1S$ waves are so narrow that, being centered on neighboring chains, they virtually do not overlap (see, as an illustration, Fig. 2), and the wave field at the exit surface of the foil can indeed be represented in the form (1), disregarding the overlap integrals, and the dynamic electron diffraction pattern can be represented in the form (2).

To calculate the Fourier transform of the wave ψ_{1S}, in Eq. (2) we use the fact that

$$\tilde{\psi}_S(k) = 2\pi \int_0^\infty r dr J_0(kr) e^{-2r/\rho} = \frac{4\pi\rho^2}{(4+k^2\rho^2)^{3/2}}, \tag{7}$$

where $k^2 = k_x^2 + k_y^2$.

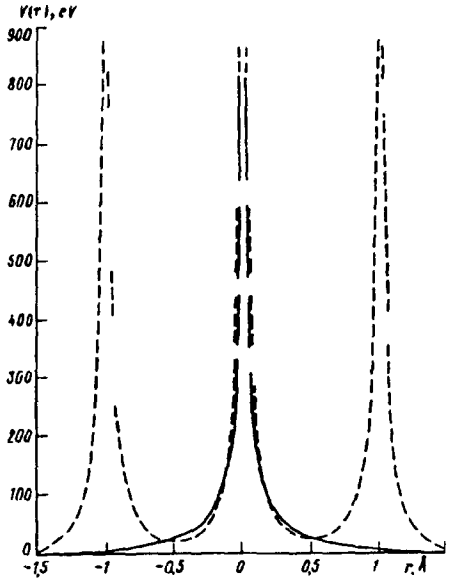

FIG. 2. Gold, 100 keV, transmission along ⟨001⟩. The parameter $\rho \approx 0.25$ Å . A small overlapping of the chain $1S$ waves (3) can be clearly seen. To construct a single $1S$ wave, it is necessary to calculate the overlap integrals and to use the tight-binding theory instead of (1).

Now, we can construct the Patterson function by Fourier transforming[1)] the intensity distribution $|\tilde{\psi}(k_x, k_y)|$ in the electron diffraction pattern and not the wave field $\psi(k_x, k_y)$. Antinodes of $\varphi(r)$

$$\varphi(r) = (2\pi)^{-1} \int_0^\infty k dk J_0(kr) |\tilde{\psi}_{1S}|^2 = \frac{\pi}{4} r^2 K_2\left(\frac{2r}{\rho}\right), \tag{8}$$

where the radius r is measured from a site of the regular Patterson lattice, will appear at the sites of the lattice described by the Patterson function. Hence we obtain for the half-width of $\varphi(r)$ the estimate $2^{2/3}\pi^{-1/3}\rho$, i.e., 0.27 Å in the case of gold. This corresponds to a half-width of the intensity peaks in the mapping of the Patterson function $\varphi^2(r)$ of the order of 0.135 Å, which is 15 times better than the resolution of good microscopes (2 Å) and approximately 40 times better than the resolution of a standard high-resolution microscopes (5 Å), to say nothing of the fact that the high-resolution microscopes are inaccessible to most experimenters.

We note, however, that we are talking about resolving atoms in a regular crystal lattice. The question of resolving lattice defects (see, for example, Ref. 2) requires an additional investigation. Here it will be necessary to distinguish the true maxima and the spurious "ghosts" in the Patterson function.

[1)]This Fourier transform of the diffraction pattern can be obtained by diffracting a laser beam on the diffraction pattern and the Patterson function with its antinodes $\varphi(r)$, which simulate the atoms in the crystal lattice, can

be visualized.

[1]F. Fujimoto, S. Takagi, K. Komaki *et al.*, Rad. Effects **12**, 153 (1972).
[2]V. L. Indenbom and S. B. Tochilin, Kristallografiya **32**, 586 (1987) [Sov. J. Crystallogr. **32**, 341 (1987)].
[3]V. L. Indenbom and S. B. Tochilin, Kristallografiya **32**, 1353 (1987) [Sov. J. Crystallogr. **32**, 795 (1987)].
[4]V. L. Indenbom and S. B. Tochilin, Zh. Éksp. Teor. Fiz. **98**, 1402 (1990) [Sov. Phys. JETP **71**, 782 (1990)].
[5]S. A. Vorob'ev, *Transmission of β-Particles Through Crystals* [in Russian], Atomizdat, Moscow, 1975.
[6]V. L. Vergasov in *Electron Diffraction Possibilities and Limitations. Abstracts of the 31st Course* (Autumn School, Halle) Saale, 1990.

Translated by M. E. Alferieff